Journal of Power Sources 236 (2013) 158–162

Contents lists available at SciVerse ScienceDirect

Journal of Power Sources

journal homepage: www.elsevier.com/locate/jpowsour

Short communication

Effect of electric potential on hydrogen adsorption over activated carbon separated by dielectric TiO_2 nanoparticles

Zheng Zhang [a,b], Jiann-Yang Hwang [a,*], Chienyu Wen [a], Xuan Li [c]

[a] Department of Materials Science and Engineering, Michigan Technological University, Houghton, MI 49931, USA
[b] Chinese Academy for Environmental Planning, Beijing 100012, China
[c] National Institute of Clean-and-Low-Carbon Energy, Beijing 102209, China

HIGHLIGHTS

- H_2 adsorption over TiO_2-coated activated carbon under electric field was studied.
- Adsorption enhancement increased with increasing amount of TiO_2.
- Dielectric TiO_2 holds more charges in each carbon particle with applied potential.
- Electrostatic force between H_2 molecule and adsorbent can be built due to charges.

ARTICLE INFO

Article history:
Received 18 August 2012
Received in revised form
30 January 2013
Accepted 12 February 2013
Available online 26 February 2013

Keywords:
Adsorption
Hydrogen
Electric potential
Carbon
Dielectric coating

ABSTRACT

This study investigates the performances of hydrogen adsorption on activated carbon separated by TiO_2 nanoparticles with the presence of an electric potential. Four species with different TiO_2 contents were prepared. Hydrogen adsorption measurements on those TiO_2-coated materials, with or without an external electric field, were made, respectively. The results showed that the adsorption capacity could be enhanced by introducing the electric potential and the enhancement increased with increasing amount of TiO_2 nanoparticles. The hydrogen adsorption capacity on TiO_2 particles is negligible, and thus there is no increase in hydrogen adsorption on TiO_2 particles alone when an electric field is applied. The effect of the dielectric coating is demonstrated.

1. Introduction

Worldwide energy crisis and environmental problems make hydrogen a prospective green energy carrier. However, the practical application of hydrogen is limited by the lack of a convenient and cost-effective method to store hydrogen [1]. Several hydrogen storage methods have been investigated, including compression, liquefaction, chemical and metal hydrides, and adsorption on porous materials [2–6]. Among them, hydrogen adsorption on activated carbon has attracted most attentions due to its low cost, abundance in supply, high porosity and surface area, and also good chemical stability [3]. It is reported that exceptionally high hydrogen storage capacities of up to 7 wt.% at 77 K have been obtained over porous carbon [7]. However, the highest storage value is still below 1 wt.% at 298 K and 100 bar, even at very high specific surface area that exceeds 3700 $m^2 g^{-1}$ [8]. The weak physisorption between hydrogen and the surface of carbon materials can be ascribed to the reason for the low storage capacity at ambient temperature.

Hybrid materials composed of nanostructured carbon and metal or metal oxide nanoparticles have been widely studied as adsorbents for hydrogen adsorption [8–13]. Experimental and theoretical results indicated that these novel hybrid materials exhibit non-classical s–p–d hybridization and spillover phenomena, resulting in increased hydrogen storage capacity [10–14].

Recently, our group has proposed a novel way to increase the hydrogen adsorption capacity on carbonaceous materials and metal oxides by introducing an electric field [15–19]. A computational work done by Liu et al. also supported the idea that imposition of an electric field could have a positive impact on hydrogen storage over graphenes [20]. Under electric field, hydrogen might be polarized or dissociated and form a stronger interaction than van der Waals

* Corresponding author. Fax: +1 906 487 2921.
E-mail address: jhwang@mtu.edu (J.-Y. Hwang).

0378-7753/$ – see front matter © 2013 Elsevier B.V. All rights reserved.
http://dx.doi.org/10.1016/j.jpowsour.2013.02.042

with charged adsorbents [18]. As carbon is electrically conductive, the induced charges would distribute onto the layer of sample surface, resulting in a limited region where strong interactions take place.

To develop an efficient storage system, we introduce TiO_2 nanoparticles into activated carbon and subsequently test hydrogen adsorption of the obtained materials under electric potential. TiO_2 is well known as an excellent dielectric material [21]. The addition of its particles may isolate the carbon particles and help to hold induced charges on each carbon particle, and thus enlarge the area with charges under electric field. Through this way, more hydrogen is expected to be tightly bonded with the adsorbent, leading to adsorption improvement.

2. Experimental

2.1. Materials

The activated carbon used in all the experiments was a commercial product of Norit Americans Inc. (denoted as NAC), with a Brunauer–Emmett–Teller (BET) surface area of 1836.2 $m^2\ g^{-1}$ and an average particle size of 20 μm. A commercial premix of TiO_2 powder (200 nm average diameter) dispersed in aqueous polyacrylic solution with propylene glycol, ester-alcohol, and ethylene glycol as stabilizer (Colorplace, Walmart). This premix is denoted as PTP (Premix TiO_2 powder). PTP contains 10% TiO_2, 33% organics and 57% water.

2.2. Sample preparation

A standard solution was first prepared by adding 5.0 g PTP into 500 ml pure ethanol and magnetically stirring for 20 min. Then 10 ml, 50 ml, 100 ml and 150 ml standard solutions, which contained 0.01 g, 0.05 g, 0.1 g and 0.15 g TiO_2 respectively, were taken out to mix with 1.0 g NAC. Ultrasonication was used to ensure the distribution of TiO_2 particles on NAC. Next, the obtained cloudy liquids were heated, accompanied by stirring, to promote volatilization until thick slurries formed. The obtained slurries were dried at 105 °C overnight to remove the solvents (water and ethanol) and other volatiles. The dried samples were denoted as P1, P2, P3 and P4. The residual organics were removed by heating P4 at 300 °C for 2 h (referred to as P4H1). For contrast, dehydrated PTP (denoted as PTPD) was prepared by dried PTP at 105 °C overnight.

2.3. Characterizations

X-ray diffraction (XRD) was carried out using a Scintag XDS2000 powder diffractometer at a scan rate of 0.08° S^{-1} with Cu radiation at 45 kV, 35 mA. A Hitachi S-4700 field emission-scanning electron microscope (FE–SEM) was used to examine the microstructure of the samples with accelerating voltage of 10 kV. The surface area was measured with a Micromeritics ASAP2000 instrument using nitrogen adsorption at liquid nitrogen temperature (77 K). The electrical resistivity was tested by a digital multimeter (Agilent 34405 A) with around 500 mg of sample powder loosely placed inside a specially designed sample holder, as shown in Fig. 1 [22].

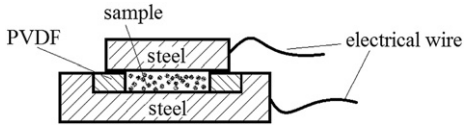

Fig. 1. Section view of sample holder used for resistivity test.

2.4. Hydrogen adsorption

Hydrogen adsorption measurements were conducted with an automatic Sievert's instrument (PCT-Pro 2000, Hy-Energy, LLC) based on static volumetric principle within 0–80 bar under room temperature (22 ± 0.8 °C). The sample holder has been modified for introducing an electric potential to the testing material, which has been shown in previous work [15]. The upper end of the sample holder was grounded and the lower end was connected to a high voltage DC power supply device, RLPS100-100P manufactured by Del Electronics Corporation. Prior to the test, the samples were dried in an oven at 105 °C for 12 h and then moved into the sample holder and evacuated at 100 °C for 2 h to ensure the removal of any contaminations from the sample surface. Around 300 mg sample was used in each run. Ultrapure (99.99999%) hydrogen and helium gases were used for all calibrations and measurements. A blank test was performed to exclude possible adsorption of hydrogen on the inner wall of the sample holder.

3. Results and discussion

3.1. Characterization

XRD patterns of P1, P2, P3 and P4 samples are shown in Fig. 2. For comparison, PTP was annealed at 500 °C for 2 h to remove water and organics thoroughly. XRD analysis of the residues only shows sharp rutile peaks (Fig. 2e). According to the ingredient list, the TiO_2 contents in P1, P2, P3 and P4 are calculated as 0.92 wt.%, 3.97 wt.%, 6.75 wt.% and 8.81 wt.%, respectively. It is obvious that the peaks of TiO_2 become sharper as the TiO_2 content increases. No other peaks are found.

Fig. 3 shows an SEM image of the P4 sample. It can be seen that the TiO_2 particles coated on the carbon surface are in tetragonal prism or tetragonal pyramid form with uniform size around 200 nm.

BET surface areas of the prepared samples are listed in Table 1. As shown in the table, only a slight reduction in surface area was observed for P1 and further addition of TiO_2 led to a sharp decrease. As for P3 and P4, the surface areas were 896.2 $m^2\ g^{-1}$ and 719.8 $m^2\ g^{-1}$, which were 48.8% and 39.2% of that of pristine NAC.

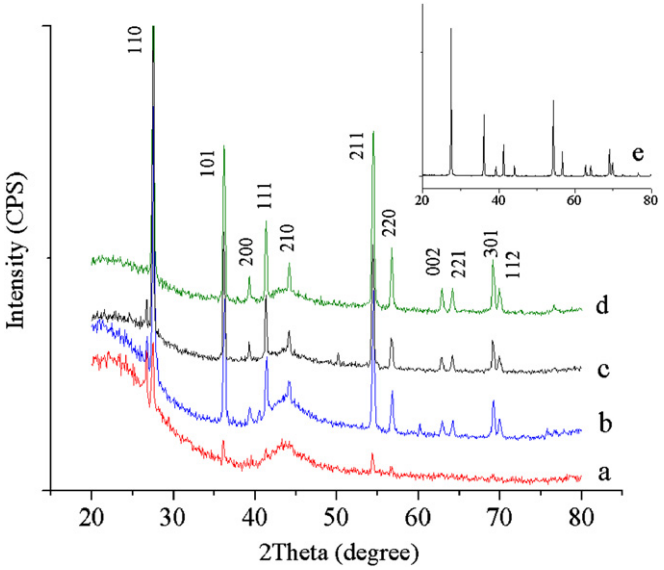

Fig. 2. XRD patterns of (a) P1, (b) P2, (c) P3, (d) P4 and (e) PTP after annealing at 500 °C for 2 h.

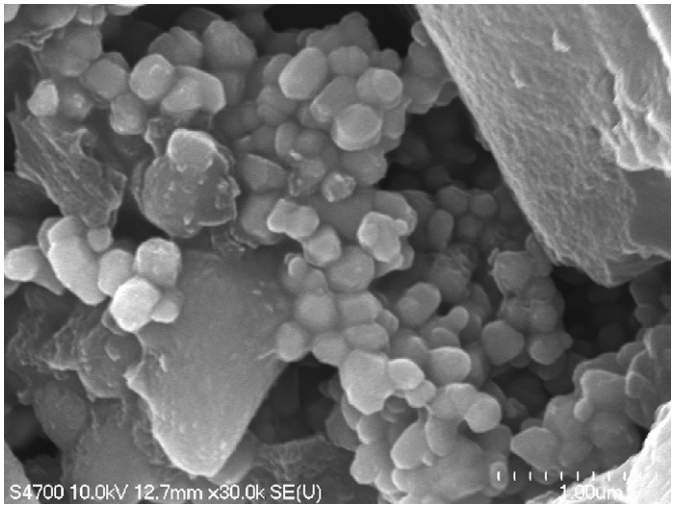

Fig. 3. FE–SEM image of sample P4.

Table 2 gives the resistivities of the synthesized hybrid samples. It is indicated that resistivity increases with the rising TiO_2 content. It is known that the addition of insulating material into a conductive matrix would raise the resistivity of the matrix. Here, rutile particles and the organic substance work together as the dielectric phase to isolate carbon particles. However, the addition of dielectric materials would largely decrease the surface area of the composite and adversely affect a relative high storage capacity. A conductor–insulator transition state, which can not only offer the ideal charged zone but also enough available sites for hydrogen adsorption, may be preferable.

3.2. Hydrogen adsorption

The hydrogen adsorption isotherms of prepared TiO_2/NAC complex in the absence of an electric field are shown in Fig. 4. For comparison, the measurement of pristine NAC is also included. The weight percentage of hydrogen adsorption shown here was obtained from the net amount of uptake after subtraction of the uptake on the blank container measurement. The data points are averaged based on three repeated experiments and the error bars represent the standard error, which is around 3% for the measurements without electric potential. It is found from the data that hydrogen uptake almost increased linearly with the growing pressure, while dropped remarkably with increasing TiO_2 content. At 80 bar, the hydrogen storage capacity of NAC was 0.43 wt.%, while uptakes of P1, P2, P3 and P4 were 0.38 wt.%, 0.25 wt.%, 0.20 wt.% and 0.19 wt.%, respectively. Moreover, we tested hydrogen adsorption over dehydrated PTP under the same conditions and found negligible storage capacity, which can be responsible for the reduced adsorption over the synthetics.

Table 1
BET surface areas of samples.

Sample identification	BET surface area ($m^2\ g^{-1}$)
NAC	1836.2
PTPD	1.9
P1	1787.2
P2	1167.0
P3	896.2
P4	719.8
P4H1	620.0

Table 2
Electrical resistivity of prepared synthetics.

Sample	P1	P2	P3	P4
Resistivity	0.035 MΩ	2 MΩ	20 MΩ	>50 MΩ

MΩ = million ohms.

An electric potential of 2000 V was then introduced to the testing sample and the results are shown in Fig. 5. Fig. 5a–d corresponds to adsorption on P1, P2, P3 and P4, respectively. Measurements for samples without potential are also included for comparison. Standard error is about 5% for the tests with potential. For sample P1, estimation of change is difficult because of the overlap of error bars of the two data sets. In Fig. 5b, a slight increment can be easily seen for P2, a sample with higher TiO_2 content. As for P3 in Fig. 5c, the gap between the two data lines becomes larger, which indicates a significant increase. Fig. 5d shows much greater improvement for P4 with the presence of electric potential. At 80 bar, the adsorption capacities for P2, P3 and P4 were 0.30 wt.%, 0.26 wt.% and 0.29 wt.% and corresponding increases were 20%, 37% and 53%, respectively, indicating growing increases as TiO_2 content rises. It should be noted that the dehydrated PTP alone has little adsorption. Such adsorption increases are considered to occur on the activated carbon.

As the surface area of the complex varies greatly, it is insufficient to simply compare hydrogen uptakes over those samples. Normalization of the adsorption capacity by the BET surface area was employed and the results are shown in Fig. 6. It is clear that application of an electric field enabled more hydrogen to be adsorbed on unit area for P2, P3 and P4. Among all the results, P4 under 2000 V voltage had the highest normalized uptake. Additionally, under an electric field the amount of hydrogen adsorbed on equivalent area increased with the increasing TiO_2 content in the sample.

A higher storage capacity is believed due to larger adsorption energy. Adsorption of hydrogen over adsorbent materials depends on three kinds of interactions: van der Waals force, electrostatic interaction and orbital interaction. Among them, van der Waals force is the weakest one [23]. The adsorption process between carbon and hydrogen is primarily weak van der Waals attraction between the π bonds of aromatic rings and the σ bonds of hydrogen

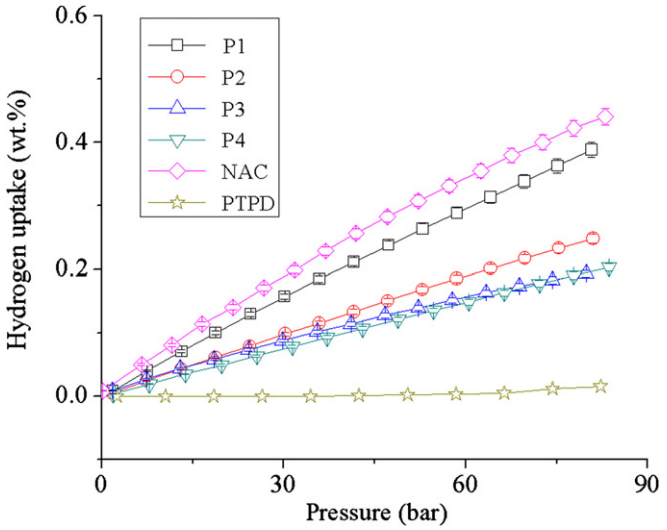

Fig. 4. Hydrogen adsorption on TiO_2/NAC synthetics (P1, P2, P3 and P4), NAC and dehydrated PTP.

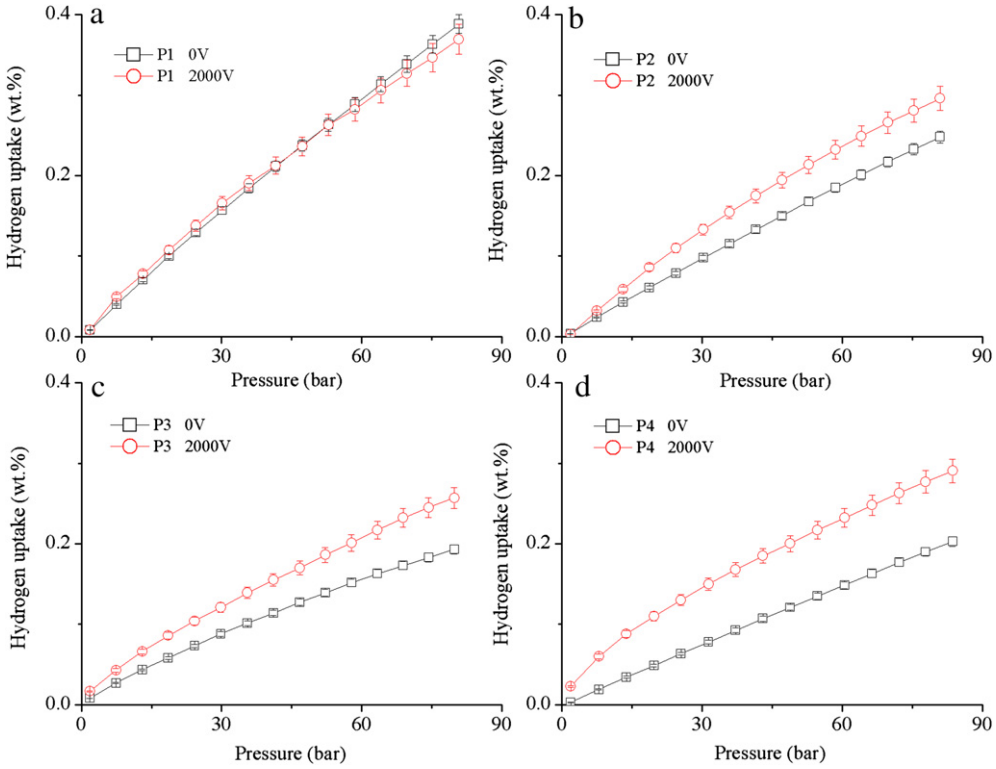

Fig. 5. Hydrogen adsorption on TiO_2/NAC synthetics (P1, P2, P3 and P4) with and without a 2000 V electric potential.

molecules. After coating activated carbon with TiO_2 particles, hydrogen molecules may dissociate and migrate onto carbon host, which is called spillover [12]. However, the supported TiO_2 particles are relatively large and poorly distributed, and thus largely limit spillover [24]. Moreover, according to the work of Lim et al. [25], spillover induced chemisorbed hydrogen only takes up 25% of total hydrogen captured on carbon/TiO_2 composite, and half is weakly chemisorbed. It is thus considered that the spillover effect can be ignored in this case and physisorption based on van der Waals force still plays the leading role. When an electric potential is applied, dielectric TiO_2 coated on carbon surface will be polarized and induced charges can be generated on carbon. The coating allows charges induced to stay at the interface of carbon particles and dielectric materials, resulting in an enlarged charged zone. Hydrogen molecules and charged carbon surface can then build electrostatic interactions, which are stronger than van der Waals forces. Shi et al. [17] also mentioned that orbital defects may be produced in adsorbent with an applied electric field, resulting in intensified orbital interactions.

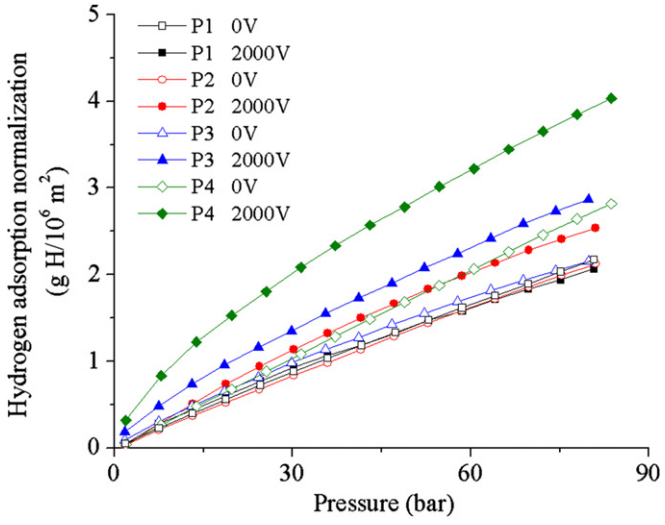

Fig. 6. Hydrogen adsorption normalized by BET surface area.

As TiO_2 content varied in species, carbon particles were isolated at different levels, or in other words, charged zones were in different sizes. Resistivity is a reflection of isolation. Higher resistivity corresponds to better isolation. On the other hand, the sample holder can be treated as a capacitor with applied electric potential. The relationship of related parameters in a capacitor can be expressed using the following equations

$$C = \varepsilon_r \varepsilon_o \frac{S}{d} \quad (1)$$

$$Q = CV \quad (2)$$

where C is the capacitance, ε_r is dielectric constant of the material between the two electrodes of the capacitor, ε_o is the electric constant ($\varepsilon_o \approx 8.854 \times 10^{-12}$ F m^{-1}), S is the area of overlap of the two electrodes, d is the separation of the electrodes, Q is the amount of induced charges and V is the electric potential applied. The dielectric constant of the complex rises with a growing ratio of dielectric materials until conductor–insulator transition is approached [26]. With other conditions unchanged, more charges would be generated as TiO_2 content goes up. Therefore, both the enlarged charged zone and increased charge amounts are responsible for more intensified hydrogen polarization, leading to improved hydrogen adsorption increase on P2, P3 and P4 samples.

As organics included in the premix rarely show good dielectric properties, TiO_2 was considered to be the dominating active

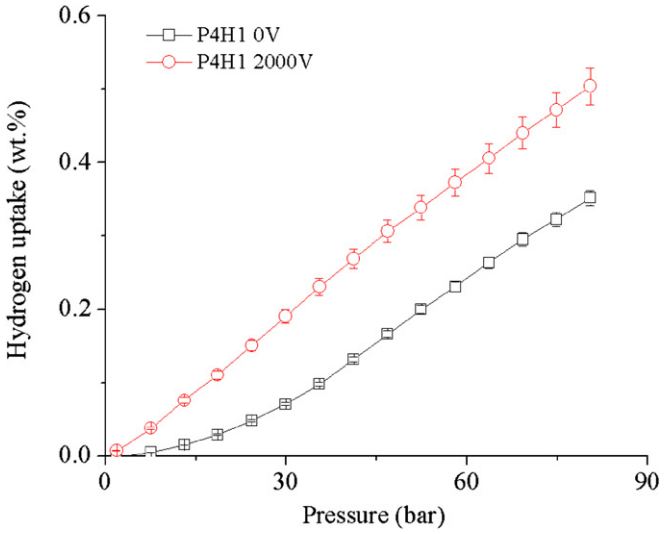

Fig. 7. Hydrogen adsorption on sample P4H1 with and without a 2000 V electric potential.

ingredient for the adsorption improvement and our further experiments confirmed the point. The organics were removed by heating the sample at 300 °C, which is a temperature higher than boiling points of all the organics. However, increase was observed as well when adsorption measurements were conducted on the heated sample, as shown in Fig. 7. With applied field, hydrogen adsorption on P4H1 at 80 bar was 0.50 wt.%, corresponding to a 47% increase. It is also noted that the storage capacity of P4H1 with an electric field at 80 bar was even higher than that of NAC (0.43 wt.%). Actually, the removal of materials with poor storage capacity greatly contributed to the increased hydrogen adsorption. Previous studies using pristine carbon as an adsorbent showed an adsorption increase of 18% at 80 bar with 2000 V electric potential [15]. Here measurements over the hybrid samples obtained the largest increase of over 50% under the same condition, twice higher than that of the carbon sample.

4. Conclusions

We developed a hydrogen storage system and demonstrated that introducing an electric field to the synthesized TiO_2/NAC hybrid materials could efficiently improve hydrogen adsorption. Storage capacities of 0.30 wt.%, 0.26 wt.% and 0.29 wt.% were obtained at 80 bar by applying 2000 V electric potential to samples with TiO_2 contents of 3.97 wt.%, 6.75 wt.% and 8.81 wt.%, corresponding to increases of 29%, 37% and 53%, respectively. No obvious improvement was observed for the sample with 0.92 wt.% TiO_2. Normalized adsorption by the BET surface area further revealed that, under an electric field, the amount of hydrogen adsorbed on a specific area increased with increasing TiO_2 content. The addition of dielectric TiO_2 to carbon isolates carbon particles, resulting in an enlarged charged zone and increased charges with applied electric field. The charges are responsible for stronger interaction between hydrogen and the solid surface. The findings from this work indicated a potential for developing high-capacity hydrogen storage system and further studies will focus on optimization of the properties and distribution of the dielectric phase.

Acknowledgement

This work was supported by the U.S. Department of Energy's Hydrogen Program, under Award Number DE-FG36-05GO15003.

References

[1] S. Shi, J.Y. Hwang, Int. J. Hydrogen Energy 32 (2007) 224–228.
[2] A.C. Dillon, M.J. Heben, Appl. Phys. A Mater. Sci. Process. 72 (2001) 133–142.
[3] Y. Yürüm, A. Taralp, T.N. Veziroglu, Int. J. Hydrogen Energy 34 (2009) 3784–3798.
[4] Y.H. Hu, L. Zhang, Adv. Eng. Mater. 22 (2010) E117–E130.
[5] R.Z. Ma, Y. Bando, H.W. Zhu, T. Sato, C.L. Xu, D.H. Wu, J. Am. Chem. Soc. 124 (2002) 7672–7673.
[6] J. Graetz, Chem. Soc. Rev. 38 (2009) 73–82.
[7] Z. Yang, Y. Xia, R. Mokaya, J. Am. Chem. Soc. 129 (2007) 1673–1679.
[8] L.F. Wang, R.T. Yang, Energy Environ. Sci. 1 (2008) 268–279.
[9] A. Lueking, R.T. Yang, Appl. Catal. A Gen. 265 (2004) 259–268.
[10] A. Mishra, S. Banerjee, S.K. Mohapatra, O.A. Graeve, M. Misra, Nanotechnology 19 (2008) 445607–445613.
[11] S. Rather, N. Mehraj-ud-din, R. Zacharia, S.W. Hwang, A.R. Kim, K.S. Nahm, Int. J. Hydrogen Energy 34 (2009) 961–966.
[12] A. Lueking, R.T. Yang, J. Catal. 206 (2002) 165–168.
[13] T. Yildirim, S. Ciraci, Phys. Rev. Lett. 94 (2005) 175501–175504.
[14] G.M. Psofogiannakis, G.E. Froudakis, J. Phys. Chem. C 113 (2009) 14908–14915.
[15] X. Li, J.Y. Hwang, S. Shi, X. Sun, Z. Zhang, Carbon 48 (2010) 876–880.
[16] X. Li, J.Y. Hwang, S. Shi, X. Sun, Z. Zhang, Fuel Process. Technol. 91 (2010) 1087–1089.
[17] S. Shi, J.Y. Hwang, X. Li, X. Sun, Energy Fuels 23 (2009) 6085–6088.
[18] S. Shi, J.Y. Hwang, X. Li, X. Sun, B.I. Lee, Int. J. Hydrogen Energy 35 (2010) 629–631.
[19] X. Sun, J.Y. Hwang, S. Shi, J. Phys. Chem. C 114 (2010) 7178–7184.
[20] W. Liu, Y.H. Zhao, J. Nguyen, Y. Li, Q. Jiang, E.J. Lavernia, Carbon 47 (2009) 3452–3460.
[21] M.D. Stamate, Thin Solid Films 371 (2000) 246–249.
[22] Z. Zhang, J.Y. Hwang, C. Wen, X. Li, Int. J. Hydrogen Energy 37 (2012) 16018–16024.
[23] R.C. Lochan, M. Head-Gordon, Phys. Chem. Chem. Phys. 8 (2006) 1357–1370.
[24] T. Sheng, X. Li, K. Yang, Acta Phys. Chim. Sin 3 (1987) 653–657.
[25] S.H. Lim, J. Luo, Z. Zhong, W. Ji, J. Lin, Inorg. Chem. 44 (2005) 4124–4126.
[26] K. Ahmad, W. Pan, S.L. Shi, Appl. Phys. Lett. 89 (2006) 133122–133124.